Complex Photophysics of the Single Tryptophan of Porcine Pancreatic Phospholipase A_2, Its Zymogen, and an Enzyme/Micelle Complex†

Richard D. Ludescher,‡,§,‖ Johannes J. Volwerk,§ Gerard H. de Haas,⊥ and Bruce S. Hudson*,‡,§

Department of Chemistry and Institute of Molecular Biology, University of Oregon, Eugene, Oregon 97403, and State University of Utrecht, Utrecht, The Netherlands

Received July 1, 1985

ABSTRACT: The fluorescence emission of the single tryptophan in porcine pancreatic phospholipase A_2, its zymogen, and a micellar complex of the enzyme with the nonhydrolyzable substrate analogue *n*-hexadecylphosphocholine has been studied by both steady-state and time-resolved techniques. Stern–Volmer quenching studies with acrylamide indicate that, both in the enzyme and in the zymogen, the tryptophan is exposed to solvent. Similar studies with ionic quenchers show that there is appreciable ionic character to the tryptophan environment. Single photon counting fluorescence measurements were performed using a high repetition rate synchronously pumped dye laser as a light source. When tryptophan fluorescence is collected with a broad-band (80-nm) emission filter, the decay kinetics in the enzyme and the zymogen require at least three, and often four, exponential terms for a proper description. The decay kinetics can be adequately described by three exponential terms when the fluorescence is collected at specific wavelengths by using narrow (10-nm) band-pass filters. The lifetimes are approximately constant across the emission band, but the amplitudes vary with the fraction of the long lifetime increasing at longer emission wavelengths. Formation of a complex between phospholipase A_2 and micelles of *n*-hexadecylphosphocholine produces large changes in the tryptophan emission that are associated with transfer to a hydrophobic environment. The decay kinetics of tryptophan in the enzyme/micelle complex appears to require only two exponential terms. This is the first reported instance of fluorescence data from a single tryptophan protein requiring more than double-exponential decay kinetics. The results are discussed in terms of the range of environments sampled by the tryptophan residue and the resulting distribution of lifetimes.

Phospholipase A_2 (phosphatide acylhydrolase; EC 3.1.1.4) (PLA_2)[1] catalyzes the stereospecific hydrolysis of the 2-acyl ester bond of 3-*sn*-phosphoglycerides. The pancreatic enzyme is synthesized as a precursor, prophospholipase A_2, of M_r 14600. The zymogen is converted to the fully active M_r 13800 enzyme by proteolytic cleavage of a seven amino acid fragment from the N-terminus. Although both proPLA_2 and PLA_2 can hydrolyze monomeric phospholipids, the processed enzyme has the interesting property that it is much more active on lipids organized into aggregates (micelles or monolayers). The activity of PLA_2 toward organized lipids can be up to 1000-fold greater than toward monomeric lipids. Several hypotheses have been proposed to explain this rate enhancement (Brockerhoff, 1968; Roberts et al., 1977; Wells, 1978; Tinker et al., 1980). The "interface recognition site" hypothesis (Verger et al., 1973; Brockerhoff, 1973; Pieterson et al., 1974) is in good agreement with current experimental data for the pancreatic enzymes. This model proposes that there is a region on the protein surface, distinct from the active site, that is involved in binding to a lipid–water interface. Formation of a complex with a lipid surface is believed to induce architectural changes at the active site that result in a more efficient enzyme. Within the context of this model the processing of the zymogen into the active enzyme involves the exposure of an interfacial binding region on the protein [see Volwerk & de Haas (1982) for a recent review].

Dijkstra et al. (1981a) have identified a ring of apolar residues on the protein surface surrounding the active site that may play a role in the interaction of pancreatic PLA_2 with lipid–water interfaces. These residues include the only tryptophan (Trp-3) in the protein. This residue is highly conserved in mammalian PLA_2. Semisynthetic studies (Slotboom & de Haas, 1975; Slotboom et al., 1978; Jansen, 1979) have shown that the apolar side chain of Trp-3 is essential for interfacial binding and catalytic activity toward organized substrates. Earlier work (Van Dam-Mieras et al., 1975) indicates that there are dramatic changes in the tryptophan absorption and emission upon binding to micellar substrates. The effects are consistent with the transfer of Trp-3 from an aqueous to a hydrophobic environment.

The presence of the intrinsic tryptophan fluorophore in proteins can provide useful information about protein structure and dynamics. The complex photophysics of the indole chromophore, however, complicates the analysis of tryptophan fluorescence in proteins [for reviews, see Weinryb & Steiner (1971), Longworth (1971), Lumry & Hershberger (1978), and

† This study is abstracted from the Ph.D. dissertation of R.D.L., who was a National Institutes of Health predoctoral trainee (GM07759) during the course of this work. This work was supported by National Institutes of Health Grants GM26536 (B.S.H.) and GM25698 (J.J.V.).

* Address correspondence to this author at the Department of Chemistry.

‡ Department of Chemistry.

§ Institute of Molecular Biology.

‖ Present address: Department of Biochemistry, The University of Minnesota Medical School, Minneapolis, MN 55455.

⊥ State University of Utrecht.

[1] Abbreviations: $C_{16}PN$, *n*-hexadecylphosphocholine; FWHM, full width half-maximum; HSA, human serum albumin; KD*P, potassium dideuterium phosphate; LSIR, least-squares iterative reconvolution; MCA, multichannel analyzer; NATA, *N*-acetyltryptophanamide; PLA_2, porcine pancreatic phospholipase A_2; PMT, photomultiplier tube; pro-PLA_2, porcine pancreatic prophospholipase A_2; TAC, time to amplitude converter; Trp, tryptophan; M_r, molecular weight.

0006-2960/85/0424-7240$01.50/0

Lakowicz (1983)]. This complexity is exemplified by the decay of the total intensity. Time-resolved measurements of single tryptophan proteins demonstrate that the tryptophan fluorescence is at least double exponential (Grinvald & Steinberg, 1976; Hazan et al., 1976; Cockle & Szabo, 1981; Ross et al., 1981a; Szabo et al., 1983). Recent studies of tryptophan as the free amino acid report that the decay is double exponential and pH dependent (Szabo & Rayner, 1980; Petrich et al., 1983); the decay may even be triple exponential in the pH region 7–10 (Gudgin et al., 1981). Complex decay kinetics are also observed for several tryptophan derivatives. In agreement with previous studies of quantum yields [e.g., see Cowgill (1963)], the values of the lifetimes are dependent both on pH and on the nature of the substituents on the α carbon (Chang et al., 1983). *N*-Acetyltryptophanamide in aqueous solution appears to represent the unusual case of a single exponential decay.

In keeping with the spirit of these recent studies, we report here that the decay of the total fluorescence intensity of the single tryptophan both in proPLA$_2$ and in PLA$_2$ is at least triple exponential and may require four, or even more, exponential terms for a satisfactory description. In a related paper (Ludescher et al., 1986), we report the results of steady-state and time-resolved polarization anisotropy measurements of the dynamics of Trp-3 in the same proteins. The polarization study shows, among other things, that the Trp-3 residue of PLA$_2$ undergoes large amplitude internal reorientational motion. This apparently exposes the chromophore to a variety of environments with a range of fluorescence decay properties.

Materials and Methods

Sample Preparation. The zymogen of phospholipase A_2 was isolated from hog pancreas and converted into fully active enzyme by limited proteolysis as described in Niewenhuizen et al. (1974). C_{16}PN was synthesized as described in Van Dam-Mieras et al. (1975). All protein and lipid solutions were prepared in 0.1 M sodium acetate buffer, pH 6.0, with glass distilled water. Protein was stored as a lyophilized powder at −20 °C and dissolved in buffer prior to use at concentrations near 10 μM. The complex of PLA$_2$ and C_{16}PN was prepared at a detergent/protein ratio of about 500 with a final C_{16}PN concentration of 5 mM. The concentration of protein was determined from the optical density at 280 nm by using $E^{1\%}_{280}$ of 13.0 for PLA$_2$ and 12.3 for proPLA$_2$ (Van Dam-Mieras et al., 1975). Tryptophan and *N*-acetyltryptophanamide were used as purchased from Sigma Chemical Co.

Fluorescence Spectra. Fluorescence emission spectra were collected at 23 °C with an SLM-8000 spectrofluorometer (SLM Industries, Urbana, IL) interfaced to a microcomputer. Excitation was at 295 nm (slit 4 nm), and emission was scanned from 300 to 475 nm (slit 2 nm) in increments of 1 nm with a 2-s integration time. It was necessary to place a quartz depolarizer in the excitation beam to eliminate the pronounced polarization bias of the excitation monochromator. Spectra were collected as a ratio of emission to lamp reference and were corrected for the wavelength-dependent bias of the emission monochromator and photomultiplier tube by using a correction curve supplied by SLM. The validity of this procedure was confirmed by agreement with published spectral parameters for tryptophan and NATA. The wavelength of maximum emission of the corrected spectra was determined from plots of the first derivative of the emission intensity vs. wavelength. The half-width of the corrected spectra was determined by graphical analysis. Relative quantum yields were determined from the ratio of the integral of the corrected emission spectra to the integral of the corrected emission spectrum of tryptophan (pH 6.0) collected under identical conditions and normalized to the solution optical densities. For calculation of the quantum yield, Q, a value of 0.12 for tryptophan at pH 6.0 was used (Chen, 1972).

Stern–Volmer Quenching. Quenching experiments were performed on a Spex Fluorolog spectrofluorometer by using excitation at 300 nm (5-nm band-pass) with emission at 350 nm (10-nm band-pass). Aliquots from freshly prepared 2.0 M stock solutions of acrylamide (Kodak, enzyme grade), KI (Fisher, reagent grade), and CsCl (Sigma, grade I) were added to 200-μL samples of proPLA$_2$ or PLA$_2$ (10 μM) at 23 °C. The high-resolution quenching experiments plotted in the insert to Figure 1 were performed by using a 0.1 M KI stock solution. The fluorescence intensity measurements were corrected for dilution effects. Corrections were made for acrylamide absorption at 300 nm by using an extinction coefficient of 0.15 M^{-1} cm^{-1} (maximum adjustment 5% at 1.2 M acrylamide). Quenching results were plotted as the ratio of the fluorescence intensity in the absence of quencher to the intensity in the presence of quencher (F_0/F) vs. the quencher concentration. The linear region of the quenching curves were fit by linear regression (all regression coefficients were greater than 0.99), and the fit slope was equated to dynamic parameters according to a modified Stern–Volmer equation: $F_0/F = 1 + K_{sv}[Q]$, where K_{sv} is $k_q\langle\tau\rangle$.

Time-Resolved Fluorescence Measurements. Time-resolved measurements were performed by using a pulsed, high-repetition rate laser and single photon counting detection procedures. The light source was a Spectra-Physics argon ion laser mode-locked at 82 MHz that was used to synchronously pump a dye laser. Very short pulses (about 15 ps FWHM) were cavity dumped at (usually) 400 kHz from the dye laser. The red output from the dye laser (rhodamine 6G) was frequency doubled to 300 nm with an angle tuned KD*P crystal. Vertical excitation and emission polarized at the "magic angle" (54.7°) were selected by Glan-Thompson polarizers. Broad-band fluorescence was selected with a Corning 7-60 band-pass filter (transmission range 310–390; maximum 350 nm). Wavelength-resolved emission was selected with 10-nm band-pass interference filters centered at 337, 360, 380, and 420 nm. Fluorescence emission was detected with an RCA 31000M photomultiplier tube. The anode output from this PMT was amplified (LeCroy Model VV101ATS) and processed with an Ortec Model 934 constant fraction discriminator. This signal was used as a start signal for an Ortec 467 time to amplitude converter (TAC). A fraction of the 600-nm dye laser output was used to trigger a fast photodiode; the output was sent to another channel of the Ortec 934 constant fraction discriminator, delayed, and used as a stop signal for the TAC. This resulted in the collection of decays in a "backward" mode and allowed the use of 400-kHz pulsed excitation. The TAC output was sent to a Tracor Northern TN-1750 multichannel analyzer (MCA) gated for detection of single photon events. This was done by processing the amplified dynode output from the RCA 31000M PM tube with an Ortec 420 single-channel analyzer that signals the MCA to store input only when the pulse originates from a single photon event at the PMT. Typically, fluorescence decays were collected at a 20-kHz accumulation rate into 1024 channels of the MCA, resulting in a counting efficiency of 5%. The full width of the system response function is near 650 ps and is very stable. The data stored in the MCA were subsequently transferred to a DEC PDP 11/34 minicomputer for analysis. Some additional details concerning this apparatus and its performance, including its ability to resolve closely spaced components of mixtures, are

discussed elsewhere (Small et al., 1984).

Analysis of Fluorescence Decay Data. Decay parameters were extracted from the experimental decays by using two basically different analysis procedures, least-squares iterative reconvolution (LSIR) and the method of moments (MOM). The LSIR analysis program uses a nonlinear least-squares iterative procedure (Grinvald & Steinberg, 1974) that employs either the Powell search algorithm (Fletcher & Powell, 1963; Himmelblau, 1972) or the Marquadt algorithm (Marquadt, 1963; Bevington, 1969) to determine the values of parameters. Decays were fit to sums of two-, three-, four-, and five-exponential components. The adequacy of fit was evaluated by the magnitude of the decrease in χ^2 when an extra component is introduced and by an examination of a plot of the modified residuals, defined as the difference between the calculated and experimental decay at each channel divided by the square root of the experimental decay value. A fit is considered adequate when such a plot shows random deviations about zero with a mean square amplitude (χ^2) of about 1.

The LSIR programs can include a variable relative time shift between the system response function and the sample data (due to variation of the photomultiplier response function with the collected wavelength) and optimization of a stray light component with the temporal characteristics of the system response as a varied fraction of the sample data. It is also possible to vary the portion of the data included in the least-squares minimization so that early components subject to large systematic errors are not counted in the minimization. (All of the system response function is included in the calculation of the convolution integral, but the result may be compared to only part of the sample data.) It will be shown with a specific example that these technical details of the data analysis have no appreciable effect on the numerical results of the analysis.

The method of moments analysis was done by using a program developed by I. Isenberg and E. Small based on a moments analysis procedure formulated by Isenberg (Isenberg, 1973a,b; Isenberg et al., 1973). The method makes use of a procedure known as moment index displacement (MD) that corrects for many systematic errors, including stray light and a relative shift of the response function and sample decays, that exist in present day instruments (Small & Isenberg, 1976, 1977; Isenberg, 1983). With this procedure, an analysis is considered adequate when λ invariance plots are flat, there is agreement between lifetimes determined by different MD values, and analysis for an additional lifetime returns the same parameter values.

In order to test the ability of these data collection and numerical methods we have obtained data for *p*-terphenyl, a molecule with emission properties similar to that of tryptophan. A good fit is obtained for a single-exponential decay with a lifetime of 1.2 ns. The χ^2 for this fit was 1.10.

Results

Fluorescence Spectra. The results of our measurements of the fluorescence emission of tryptophan, *N*-acetyltryptophanamide, and Trp-3 in proPLA$_2$, PLA$_2$, and the complex of PLA$_2$ with the zwitterionic detergent C$_{16}$PN are summarized in Table I. The emission of tryptophan amino acid in buffer has a peak at 348 nm and a bandwidth of 57 nm. Derivatization of the amino acid to NATA has a slight effect on the emission bandwidth and causes a 2-nm red shift in the maximum. The tryptophan emission from proPLA$_2$ and PLA$_2$ differs markedly from that of the free amino acid. The maximum is shifted to higher energy (344 nm for proPLA$_2$ and 340 nm for PLA$_2$), and the bandwidth is narrower. The formation of a protein complex with C$_{16}$PN produces large changes in the tryptophan emission characteristics of PLA$_2$. The maximum shifts 7 nm to the blue (to 333 nm), and the bandwidth is 7 nm narrower. These changes in tryptophan fluorescence are usually associated with transfer to a less polar environment. Our measurements are in agreement with the findings of Van Dam-Mieras et al. (1975).

Table I: Fluorescence Emission Spectral Parameters of Tryptophan Amino Acid, NATA, and Trp-3 in PLA$_2$, proPLA$_2$, and PLA/C$_{16}$PN Micelles and Comparison with the Spectral Types of Burstein[a]

sample	emission maximum (nm)	emission bandwidth (nm)	Q^b relative	Q^c
Spectral Parameters				
tryptophan	348	57	1	0.12
NATA	350	58	0.89	0.11
proPLA$_2$	344	54	0.77	0.092
PLA$_2$	340	52	0.26	0.031
PLA$_2$/C$_{16}$PN	333	45	0.62	0.074
Tryptophan Spectral Classification[d]				
Ia buried	330–332	48–49		0.11
Ib buried	330–332	48–49		0.4–0.5
II surface: hidden	340–342	54–56		0.3
III surface: exposed	350–353	59–61		0.2

[a] Phospholipase spectral parameters are from the corrected emission spectra at 23 °C and excitation at 295 nm. All samples are in pH 6.0, sodium acetate buffer (0.1 M). The error in wavelength maximum and bandwidth is ±0.5 nm. [b] Q relative is calculated from the ratio of the corrected emission spectrum integrated with respect to wavelength (divided by the optical density at 295 nm) to that of tryptophan taken under the same instrumental conditions. [c] Q is calculated assuming a quantum yield of 0.12 for tryptophan at pH 6.0 (Chen, 1972). [d] This classification scheme associates the location of a tryptophan in a protein with the spectral parameters listed, from Burstein et al. (1973).

Table II: Stern–Volmer and Collisional Rate Constants for the Quenching of Trp-3 Fluorescence in proPLA$_2$ and PLA$_2$ at 23 °C

	proPLA$_2$		PLA$_2$		
quencher	K_{sv} (M^{-1})	k_q[a] × 10^9 (M^{-1} s^{-1})	K_{sv} (M^{-1})	k_q × 10^9 (M^{-1} s^{-1})	k_q[b] ratio
acrylamide	14.0	3.6	7.2	4.0	1.1
cesium	1.8	0.46	1.1	0.61	1.3
iodide	7.8	2.0	5.8	3.2	1.6

[a] k_q is equal to $K_{sv}/\langle\tau\rangle$; it was calculated by using the values of the average lifetime listed in Table III. K_{sv} is calculated from a linear least-squares fit to the initial region (<0.3 M quencher) of the quenching curves. The error in k_q is ±10%. [b] This is the ratio of k_q for PLA$_2$ to k_q for proPLA$_2$.

The quantum yield of Trp-3 increases about 2.4-fold when PLA$_2$ forms a complex with C$_{16}$PN (see Table I). This large increase appears to be related to an unusually low quantum yield for Trp-3 in PLA$_2$ rather than to a high quantum yield in the complex. The average value of Q (relative to 0.12 for tryptophan) for 19 proteins tabulated in Longworth (1971) is 0.12 ± 0.08. The quantum yield of Trp-3 in PLA$_2$, 0.031, is far below this average while the values for proPLA$_2$ and PLA$_2$/C$_{16}$PN are closer to the typical value.

Stern–Volmer Quenching of proPLA$_2$ and PLA$_2$. The emission spectra of Trp-3 in proPLA$_2$ and PLA$_2$ indicate that the tryptophan is exposed to solvent in both PLA$_2$ and proPLA$_2$. This was confirmed by studying the collisional quenching of Trp-3 with the neutral quencher acrylamide and two ionic quenchers, iodide and cesium. The Stern–Volmer quenching constants, K_{sv}, and the collisional rate constants, k_q, are summarized in Table II. Although probably overestimated,[2] the collisional rate constants for all three quenchers

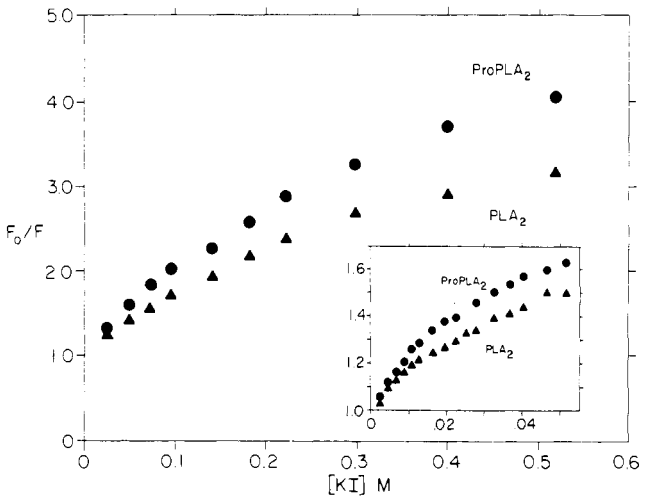

FIGURE 1: Stern–Volmer plot of the quenching of Trp-3 fluorescence in proPLA$_2$ (circles) and PLA$_2$ (triangles) by iodide. The insert is a plot of the initial portion of the curve at a constant ionic strength of 0.1 M salt (KI and KCl). Excitation at 300 nm (spectral slit width 5 nm); emission at 350 nm (spectral slit width 10 nm). The temperature was 23 °C.

appear large for both PLA$_2$ and proPLA$_2$, indicating that Trp-3 is very accessible to the quencher and presumably to the solvent as well. The difference in collisional rate for the two proteins, however, varies for each quencher. For the neutral molecule acrylamide the rate constants differ by only 10%. The difference is more pronounced in the case of the two ionic quenchers: for cesium k_q is 30% larger in PLA$_2$ than in proPLA$_2$ while for iodide k_q is 60% larger in PLA$_2$ than in proPLA$_2$. It appears that the extra seven amino acids at the N-terminal of the zymogen may provide a small steric but a large electrostatic hindrance to quencher accessibility in proPLA$_2$.

The iodide quenching of Trp-3 in both proPLA$_2$ and PLA$_2$ is illustrated in Figure 1 in a Stern–Volmer plot of F_0/F vs. iodide concentration. The Stern–Volmer quenching constants listed in Table II were calculated from the slopes of these curves. The insert in Figure 1 indicates that the initial (0–0.05 M) portion of the iodide curve is actually biphasic. There is an initial, efficient quenching region at low concentrations followed by a more gradual quenching region. The gradual quenching region has the same slope as the low-resolution curves plotted in Figure 1. This initial efficient quenching behavior is not present in 1.0 M KCl, and the acrylamide Stern–Volmer plots are linear to at least 0.6 M.

Multiexponential Emission Decay of Trp-3 in proPLA$_2$ and PLA$_2$. The time-resolved emission intensity of Trp-3 in pro-

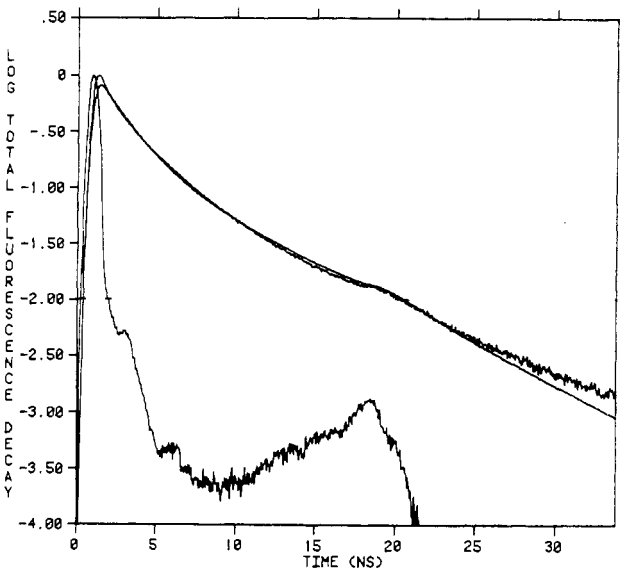

FIGURE 2: Logarithmic plot of the fluorescence of Trp-3 of proPLA$_2$ [$I(t)$] at 20 °C collected with a broad-band emission filter. The logarithm of the machine response profile [$L(t)$] is also plotted at the bottom. Excitation was at 300 nm with vertical polarization; emission polarized at 54.7° was collected through a Corning 7-60 broad band-pass filter. The smooth line is the best two-component fit to these data as discussed in the text.

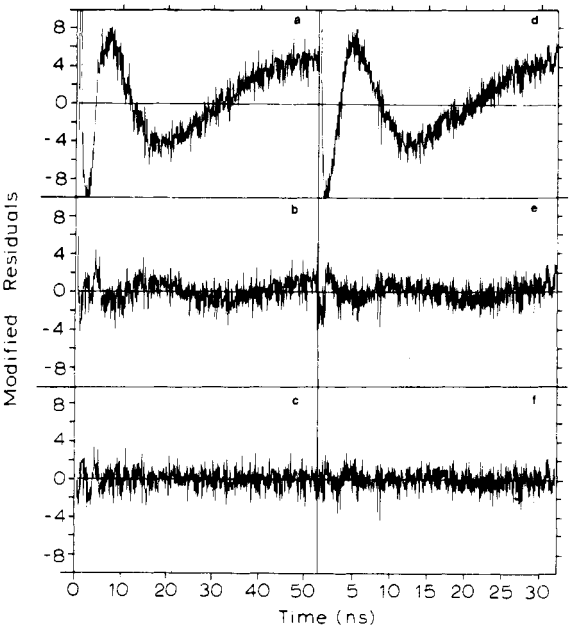

FIGURE 3: Modified residuals plots from LSIR fits to the decay of the total fluorescence of Trp-3 in proPLA$_2$ (a–c) and PLA$_2$ (d–f) at 20 °C. The plots are for fits to the emission decay using sums of two- (a and d), three- (b and e), and four- (c and f) exponential terms. Excitation was at 300 nm; emission polarized at 54.7° was collected through a Corning 7-60 broad band-pass filter.

PLA$_2$ at 20 °C collected with a broad-band emission filter is shown in Figure 2 together with a machine response function and the best-fit two-exponential decay. The peak value of the experimental data is 270 000 counts. This curve is typical of the signal-to-noise ratio of the decays collected with broad-band emission that we report here. The modified residuals from the results of a least-squares iterative reconvolution (LSIR) analysis of the decay in Figure 2 employing two, three, and four exponentials are plotted in Figure 3a–c (see figure legend for details). The large oscillation in the modified residuals plot in Figure 3a shows that the emission decay cannot be described adequately by two exponential terms. The ad-

[2] The downward curvature in the quenching curves in Figure 1 indicates that the simple Stern–Volmer model may be inadequate. If the quenched fluorophore has several lifetime components, the quenching curves are described in general by the equation

$$F_0/F[Q] = \sum_{i=1}^{n} a_i\tau_i / [\sum_i a_i(1/\tau_i + k_{qi}[Q])]$$

where i labels each lifetime component and there are n lifetimes. We have modeled the curves in Figure 1 with this equation using the four lifetime components determined by LSIR analysis (as will be discussed) and using a single value of k_q; i.e., we assume that the differential quenching of the various species is only due to the differences in lifetimes. The curves that result only reproduce the downward curvature in part. The fit values of k_q, 0.65 and 1.2×10^9 M^{-1} s^{-1} for proPLA$_2$ and PLA$_2$, show that the values listed in Table II are probably overestimates of the collisional parameters. The ratios of the collisional rates reported in Table II, however, are probably good approximations of the actual trends.

Table III: Variation of χ^2 with Number of Exponential Components for the Fluorescence Decays of $proPLA_2$ and PLA_2

	$proPLA_2$ at T (°C) =			PLA_2 at T (°C) =		
N	8	20	40	8	20	40
2	12.7	9.3	74.3	101.6	22.5	25.6
3	1.7	1.5	3.9	6.4	1.7	2.0
4	1.4	1.3	1.7	2.1	1.1	1.3
5	1.4	1.2	1.6	1.6	1.1	1.3

dition of a third term also does not result in random deviations (Figure 3b). Only a four-exponential description results in a truly random modified residuals plot (Figure 3c).

Fluorescence decays for PLA_2 obtained under similar conditions have a complexity similar to that observed for $proPLA_2$. This is illustrated in Figure 3d–f which includes plots of the modified residuals from the results of LSIR analyses using two, three, and four components. In this case also, nonrandom deviations in the three-component plot (Figure 3e) indicate that three terms are not sufficient to describe the decay. An adequate description of the decay kinetics requires at least four exponential terms (Figure 3f). LSIR analysis of emission decays of both $proPLA_2$ and PLA_2 collected at 8 and 40 °C (Table V) demonstrates that comparable excited-state decay complexity exists for Trp-3 at these temperatures. Analysis of the emission decays using the method of moments confirms that the tryptophan emission decays of $proPLA_2$ and PLA_2 are not adequately described as the sum of three exponential terms at either 8, 20, or 40 °C. We conclude that the decay of the emission of the single tryptophan in $proPLA_2$ and PLA_2 involves four or more lifetime components.

In order to make these conclusions more plausible we present a detailed analysis of some of the data. The result of incrementing the number of lifetime components on the χ^2 values for the $proPLA_2$ and PLA_2 data sets is shown in Table III. Increasing the number of lifetime components from two to three is necessary in all cases in order to obtain "satisfactory" agreement with the experiment. A four-exponential fit seems to be clearly justified in several cases, especially $proPLA_2$ at 40 °C and PLA_2 at 8 °C. In the case of PLA_2 at 20 °C χ^2 decreases from 1.7 to 1.1 on going from three to four components. This is considered to be marginally significant. Confirmation of the need for four components in this and similar cases rests primarily on the systematic behavior of the residual plots (Figure 3). Five-component analyses do not improve the χ^2 significantly relative to the four-component results although the case of PLA_2 at 8 °C is on the verge of credibility.

In order to confirm that a two-component fit could not be found that is as satisfactory as that involving three components, some of the data were analyzed with a two-component analysis with optimization of the contribution of stray light and a relative shift between the system response function and the collected data. The χ^2 value was calculated by using all of the data from the peak of the response function. The minimum χ^2 for a two-component fit obtained with optimized shift and scatter parameters for the 20 °C PLA_2 data was 14.8. A three-component fit without optimization of the scatter or shift gave a value of $\chi^2 = 4.8$ (see Table IV) and, with optimization of these factors, $\chi^2 = 1.5$. Thus, a significant improvement in χ^2 is obtained by inclusion of a third lifetime component no matter how the other features of the analysis are handled.

Another interesting aspect of these experiments is that the parameters derived for the fits do not depend appreciably on the details of the analysis method and are very reproducible from one experiment to another. The analysis of three independent experiments (all PLA_2 at 20 °C) using a variety of numerical methods is shown in Table IV. The analysis methods include use of all of the data in the calculation of χ^2, inclusion of data from the peak of the excitation pulse, inclusion of only that data after the excitation pulse has died to 10% of its peak value, and a methods of moments (MOM) analysis, all of the same data set. A second data set obtained with our apparatus is indicated in Table IV by footnote *d*. Furthermore, an entirely independent experiment has been performed by R. R. Alcala, F. P. Prendergast, and E. B. Gratton using a high-frequency phase/modulation method. A three-component analysis of this phase and modulation data is also given in Table IV. The excellent agreement observed between the values obtained by all of these analysis methods and independent repetitions of the experiment demonstrates that the results are not determined by the details of the method used.

It should be noted that the lifetimes obtained in these analyses are rather widely separated and that each component

Table IV: Comparison of Results of Three- and Four-Component Analyses for Phospholipase A_2 at 20 °C Using Different Analysis Methods[a]

method	a_1	τ_1	a_2	τ_2	a_3	τ_3	a_4	τ_4	χ^2
				Three-Component Analysis					
all data[b]	0.071	6.93	0.382	2.49	0.546	0.512			11.5
from peak[b]	0.075	6.70	0.377	2.34	0.549	0.422			4.8
from peak[b,d]	0.077	6.71	0.394	2.56	0.529	0.606			25.0
from peak[c]	0.072	7.13	0.416	2.86	0.522	0.623			2.6
10% peak[b]	0.073	7.20	0.411	2.67	0.516	0.684			1.7
10% peak[b,d]	0.079	6.84	0.410	2.66	0.511	0.712			2.7
10% peak[c]	0.064	7.56	0.416	2.86	0.520	0.774			1.4
MOM[e]	0.074	7.29	0.412	2.82	0.514	0.834			
phase[f]	0.089	6.95	0.395	2.79	0.515	0.704			
				Four-Component Analysis					
from peak[b]	0.039	7.83	0.250	3.09	0.286	1.07	0.425	0.241	2.1
from peak[b,d]	0.039	7.86	0.197	3.68	0.292	1.86	0.472	0.542	24.1
10% peak[b]	0.043	7.98	0.275	3.22	0.304	1.26	0.378	0.378	1.2
10% peak[b,d]	0.056	7.10	0.308	2.86	0.351	0.90	0.285	0.231	2.0

[a] All lifetimes in nanoseconds. "All data" means that the entire data set (1024 channels minus an initial background region) were used in the calculation of χ^2 in a least-squares iterative reconvolution calculation. "From peak" means that only the data from the peak of the excitation pulse was used in the calculation of χ^2. "10% peak" means that only the data from the point where the excitation pulse had fallen to 10% of its original value is used in the calculation of χ^2. (All data points are used in the calculation of the convolution integral in all cases.) [b] No scatter subtraction was included. [c] A variable scatter subtraction factor was included in the analysis. [d] A duplicate experiment. [e] Analysis of the original data set (all points) using the method of moments with moment index displacement MD 2 and λ suppression of 0.36 [see Isenberg (1973a,b), Isenberg et al. (1973), Small & Isenberg (1976, 1977), and Small et al. (1984)]. [f] A third independent experiment performed using phase modulation methods (E. Gratton, private communication).

Table V: Decay Components, Average Lifetimes, and Lifetime Distribution Standard Deviations for proPLA$_2$ and PLA$_2$[a]

protein	T (°C)	a_1	τ_1	a_2	τ_2	a_3	τ_3	a_4	τ_4	$\langle\tau\rangle$	S[b]
					Three-Component Analysis						
proPLA$_2$	8	0.302	9.45	0.328	4.52	0.370	1.44			4.87	3.3
proPLA$_2$	20	0.311	7.78	0.357	3.14	0.331	0.92			3.85	2.8
proPLA$_2$	40	0.054	5.61	0.419	2.03	0.527	0.60			1.47	1.2
PLA$_2$	8	0.065	8.44	0.396	3.54	0.539	0.91			2.44	2.0
PLA$_2$	20	0.073	7.20	0.411	2.68	0.516	0.68			1.98	1.7
PLA$_2$	40	0.055	5.64	0.422	2.06	0.524	0.64			1.51	1.2
					Four-Component Analysis						
proPLA$_2$	8	0.220	9.90	0.258	6.10	0.320	2.42	0.202	0.85	4.70	3.3
proPLA$_2$	20	0.239	8.12	0.264	4.11	0.303	1.52	0.195	0.40	3.56	2.9
proPLA$_2$	40	0.029	6.31	0.201	2.69	0.360	1.24	0.411	0.36	1.31	1.2
PLA$_2$	8	0.022	10.37	0.214	4.99	0.345	2.16	0.420	0.63	2.30	2.0
PLA$_2$	20	0.043	7.98	0.275	3.22	0.304	1.26	0.378	0.38	1.76	1.8
PLA$_2$	40	0.029	6.33	0.200	2.73	0.373	1.28	0.397	0.39	1.37	1.2

[a] All lifetimes in nanoseconds. [b] The standard deviation of the lifetime distribution.

Table VI: Three-Exponential Decay Components for PLA$_2$ at 20 °C for Several Emission Wavelengths[a]

emission (nm)	a_1	τ_1	a_2	τ_2	a_3	τ_3	$\langle\tau\rangle$
337	0.085 (2)	6.08 (4)	0.393 (5)	2.29 (3)	0.521 (7)	0.63 (1)	1.74
360	0.105 (3)	6.34 (6)	0.417 (10)	2.40 (5)	0.478 (11)	0.69 (3)	2.00
382	0.121 (2)	6.59 (4)	0.412 (6)	2.49 (3)	0.467 (8)	0.68 (2)	2.14
420	0.131 (5)	8.46 (10)	0.414 (6)	3.32 (7)	0.456 (10)	0.78 (3)	2.83

[a] All lifetimes in nanoseconds. The numbers in parentheses are the standard deviations derived from the least-squares fitting procedure in units of 0.001 for the amplitudes and 0.01 ns for the lifetimes.

makes a significant contribution to the total fluorescence. It is this pattern of lifetimes that makes the analysis of this complex case possible. On the other hand, a continuous distribution of lifetimes with an appreciable width would give rise to this pattern of apparent decays with well-spaced rates. This will be discussed in more detail.

Analysis of the emission decay of Trp-3 in the PLA$_2$/C_{16}PN complex suggests that again in this case at least four exponential terms are needed to describe the data. Data analysis using both LSIR and the method of moments demonstrates, however, that at 20 °C about 95% of the total emission intensity is from only two lifetime components with additional small contributions from both a very long (~20 ns) and a very short (~0.2 ns) lifetime component. The latter lifetimes are also observed in a control experiment where the emission decay of C_{16}PN micelles was collected in the absence of any protein. Both the very long and the very short components must therefore be attributed to fluorescent impurities in the detergent preparation. (The buffer solutions used for all experiments had negligible fluorescence.) We tentatively conclude that no more than two exponential terms are required to describe the decay of Trp-3 in the PLA$_2$/C_{16}PN complex. For 20 °C the decay parameters are $a_1 = 0.66$, $\tau_1 = 3.20$ ns, $a_2 = 0.34$, and $\tau_2 = 1.75$ ns. The average lifetimes at 8, 20, and 40 °C for the tryptophan fluorescence of this micelle complex are 3.7, 2.7, and 1.6 ns, respectively. Comparison of these values with those given for PLA$_2$ in Table V at these temperatures shows that the complex has significantly longer average lifetime values. This is true even though a possible long lifetime component has been rejected due to lipid fluorescence. This indicates that some quenching mechanism present in the protein is less important in the complex.

Emission Wavelength Resolved Fluorescence Decay of PLA$_2$. The complex emission decays of Trp-3 described above were all collected by using a broad band-pass filter centered at 350 nm. We have also collected emission decays of Trp-3 in PLA$_2$ at 20 °C using 10-nm band-pass interference filters. The decays at each wavelength are well described by three-exponential fits. This conclusion is derived from both method of moments analysis and LSIR determination of the value of χ^2 with increasing number of components. This apparent ability to fit these decays with only three components while the broad-band data requires four components in many cases is probably a reflection of the much smaller number of counts collected in these narrow band experiments. The resulting parameter values are given in Table VI. The average lifetime increases continuously as the emission wavelength is moved to the red edge. The individual decay times obtained in this analysis are very nearly constant across the emission band while the short and long lifetime component amplitudes decrease and increase, respectively. The amplitude of the intermediate lifetime component remains approximately constant across the emission band. The variation of average lifetime, therefore, reflects a change in the "spectrum" of decay constants, with the longer wavelength component having relatively more intensity in the longer time region.

Discussion

Steady-State Fluorescence. According to the fluorescence spectral criteria of Burstein et al. (1973), Trp-3 is on the protein surface in both proPLA$_2$ and PLA$_2$. The quenching studies with acrylamide support this conclusion. The values of k_q for both proPLA$_2$ and PLA$_2$ are near 4×10^9 M^{-1} s^{-1}, which is the value of k_q found by Eftink & Ghiron (1976) for ACTH and glucagon, two small peptides with little secondary structure. Such large values of k_q suggest that Trp-3 may be extensively exposed to solvent in both proPLA$_2$ and PLA$_2$. The crystal structure of porcine pancreatic PLA$_2$ (Dijkstra et al., 1983) places the indole ring at the protein surface in a shallow cleft between the N-terminal α-helix and one strand of a two-strand β-sheet. One face of the indole ring appears to be entirely exposed to solvent. A similar orientation for Trp-3 is found in the crystal structure of bovine PLA$_2$; this structure is nearly identical with the porcine structure and is known to higher resolution (Dijkstra et al., 1981b). The acrylamide quenching results support an orientation for Trp-3 in PLA$_2$ in solution similar to that reported for the crystal structure. The collisional quenching results also indicate considerable

solvent exposure of Trp-3 in the zymogen. The first 10 amino acids of proPLA$_2$, including Trp-3, are not visible in the crystal structure of the bovine zymogen (Dijkstra et al., 1982). The relevance of this point to dynamic disorder of the N-terminal end of proPLA$_2$ is discussed in a subsequent publication (Ludescher et al., 1986).

The efficient quenching by iodide in the low concentration region of the Stern–Volmer plot (insert to Figure 1) may be due to the presence of an iodide binding site near Trp-3. Two factors influence this interpretation. First, the quenching disappears at high ionic strength, and second, k_q for this region of the curve appears too large to be due to collisional quenching (6×10^9 and 11×10^9 M^{-1} s^{-1} for proPLA$_2$ and PLA$_2$, respectively). Similar behavior has been seen with iodide quenching of the single tryptophan in HSA (Lehrer, 1976) and was interpreted to mean that there is an iodide binding site near the tryptophan. In PLA$_2$ both Arg-6 and the α-amino group of Ala-1, which are close to Trp-3 and on the same face of the N-terminal α-helix, are possible binding sites for iodide. In proPLA$_2$, Arg-6 and Arg-(−1) are candidates. Our present data do not provide a way of distinguishing which residues are responsible.

The complex ionic environment near Trp-3 in these proteins is reflected in the difference in k_q between proPLA$_2$ and PLA$_2$ for cesium and iodide. The ratios of the collisional rate constants of proPLA$_2$ and PLA$_2$ for both the negative quencher iodide and the positive quencher cesium are larger than for the neutral quencher acrylamide. This implies that the Trp-3 environment of the two proteins differs in both negative and positive charges. It is possible that, in the zymogen, the positively charged arginine at position −1 and the negatively charged glutamic acid at position −6 provide additional electrostatic shielding of the indole ring from ionic quenchers.

Time-Resolved Fluorescence. The literature on tryptophan lifetimes in proteins contains an interesting trend. The fluorescence decay of single tryptophan proteins is often reported to be double exponential, while, with a single exception (Privat et al., 1980), the fluorescence of multi-tryptophan proteins is also reported to be double exponential. The specific values of the lifetimes vary from protein to protein. The two lifetimes reported by Grinvald & Steinberg (1976) for proteins containing a single tryptophan fall in the range from 0.3 to 2.5 ns for the short lifetime and from 2.4 to 6.1 ns for the long lifetime. The reason that only two lifetimes are reported may be due to the inherently difficult problem of extracting exponential decay parameters from real data. It is possible that the instrumental limitations of previous measurements, especially the low repetition rate, poor stability, and relatively broad bandwidth of flashlamp excitation sources, prevented the acquisition of data of sufficient time resolution and signal-to-noise to resolve three or more closely spaced exponentials. Using a high-repetition rate, pulsed laser light source, we have collected data of sufficient quality to confidently conclude that the decays of Trp-3 in proPLA$_2$ and PLA$_2$ are at least triple exponential and probably require four (or more) exponentials for a complete description.

A discussion of this multiexponential decay is complicated by the complex photophysics of indole and its derivatives. A short review will illustrate the flavor of the problem. The near-UV transition in indoles is due to two overlapping allowed transitions, $1L_a$ and $1L_b$. The stronger $1L_a$ transition is diffuse and broad and overlays the weaker $1L_b$ transition (Konev, 1967; Yamamoto & Tanaka, 1972; Valeur & Weber, 1977). Solvent polarity differentially shifts the $1L_a$ energy due to its large excited-state dipole moment (Strickland et al., 1970). Dual fluorescence from both states occurs in some indole derivatives but apparently not in tryptophan (Andrews & Forster, 1974). Stable complexes called exciplexes, which may or may not be fluorescent, can form between the excited state of the indole chromophore and many polar molecules (Walker et al., 1967; Lumry & Hershberger, 1978). There is also appreciable Rydberg character to these near-UV transitions (Lami, 1977) due to the mixing of higher energy ionizable states with, probably, the $1L_a$ state. This is related to the electron ejection that can occur when indole derivatives are excited to high vibrational levels of S_1 (Joschek & Grossweiner, 1965; Bent & Hayon, 1975). Electron loss from vibrationally relaxed excited molecules can also occur due to either intramolecular or intermolecular charge-transfer interactions with nearby electronegative groups (Feitelson, 1971). Electron loss may be the predominate temperature-dependent nonradiative decay channel for tryptophan (Kirby & Steiner, 1970), and charge-transfer reactions in conjunction with ground-state rotamers have recently been invoked to explain the double-exponential decay of tryptophan and its derivatives (Chang et al., 1983; Petrich et al., 1983). Solvent reorientation around the larger dipole moment of the $1L_a$ excited state has a pronounced effect on the Stokes shift of indole and tryptophan fluorescence and may also influence the nonradiative decay rates of these fluorophores (Eisinger & Navon, 1969). Ground-state heterogeneity, as well as mobility on the fluorescent time scale that changes the orientation and proximity of nearby chemical groups, may influence the relative contributions of all of these nonradiative pathways.

In addition to the complex photophysics of indole, there are two other factors that must be considered when the multiexponential decay of tryptophan in proteins is discussed [see Ross et al. (1981a)]. First, each lifetime species may represent a different ground-state conformer of the tryptophan. These conformers include different rotamers about the C–C bond of the tryptophan as well as different conformations of the rest of the protein. The second factor to consider is the influence of what may be loosely called excited-state reactions of the tryptophan. These include solvent or protein reorientation around the excited-state fluorophore, the formation of exciplexes, and reorientations of the chromophore during the excited-state lifetime that significantly change the environment of the indole ring.

In phospholipase A$_2$ there are several residues in the vicinity of Trp-3 that may interact with the indole ring and affect the nonradiative decay rates of tryptophan. A glutamine residue (Gln-4) is in van der Waals contact witht the indole ring in the crystal structure of bovine PLA$_2$ (Dijkstra et al., 1981b). It is not possible to determine if this is the case in porcine PLA$_2$ because of the lower resolution of the crystal structure (Dijkstra et al., 1983). Amide residues are excellent quenchers of tryptophan fluorescence and also form exciplexes with indole derivatives (Lasser et al., 1977). This glutamine residue is therefore likely a good quencher of the tryptophan residue and may explain the large fraction of nonfluorescent tryptophans that we estimate to be in these proteins (as will be discussed). The experiment that could in principle test this assumed role of Gln-4 as a quencher is the examination of a semisynthetic protein in which this residue has been replaced by another nonquenching group. This experiment has, in fact, been performed (van Scharrenburg et al., 1982). The major relevant observation concerning this modified protein with Gln-4 replaced by Nle is that the quantum yield of its fluorescence is considerably *less* (roughly, 7-fold) than that of the parent PLA$_2$. This indicates that there is even more efficient radi-

ationless decay for Trp-3 in the absence of Gln-4. The interpretation of this experiment so far as the Trp-3 photophysics is concerned is complicated by the fact that this invariant Gln-4 residue is apparently structurally important and the resulting modified protein is at least partly unfolded.

The charged amino group at the N-terminal, which is a good quencher of tryptophan fluorescence, is also close to Trp-3 in PLA_2. (It is, in fact, hydrogen bonded to Gln-4.) There is also a glutamic acid residue at position 71 on the β-sheet that is adjacent to Trp-3 and a string of alcoholic amino acids on the same β-sheet: serines at positions 72 and 74 and tyrosines at residues 73 and 75. Alcohols are known to form exciplexes with indole derivatives (Lumry et al., 1962). Disulfide groups, tyrosine, and peptide bonds are also excellent electron scavengers from excited indoles (Lumry & Hershberger, 1978). There are numerous peptide groups and two disulfide bonds near Trp-3, one connecting Cys-11 and Cys-77 and another connecting Cys-84 and Cys-96. In addition, the quenching results indicate that there is a fairly rich ionic environment in the vicinity of Trp-3. All of the above groups may potentially interact with the excited state of Trp-3. In such a complex chemical environment it is possible that small changes in the indole environment, i.e., slightly different conformations of the tryptophan, may make large changes in the nonradiative decay rate. If the indole ring is rotating rapidly with respect to the rest of the protein, then these interactions can change during the excited-state lifetime. This possibility is supported by time-resolved anisotropy studies (Ludescher et al., 1986) which show that Trp-3 does indeed rotate on the subnanosecond time scale.

The wavelength dependence of the Trp-3 lifetime amplitudes in PLA_2 provides some insight into possible explanations of the multiple tryptophan lifetimes. An increase in the amplitude of a long lifetime component as the wavelength of emission increases is also seen in tryptophan at pH 7.0 (Szabo & Rayner, 1980), in the single tryptophan protein glucagon (Cockle & Szabo, 1981) and in the multi-tryptophan proteins *Escherichia coli lac* repressor [two tryptophans (Brochon et al., 1977)], horse liver alcohol dehydrogenase [two tryptophans (Ross et al., 1981b)], and yeast 3-phosphoglycerate kinase [three tryptophans (Privat et al., 1980)]. This sort of behavior is generally explained either by the presence of multiple ground states with different emission spectra (Szabo & Rayner, 1980) such that the red-shifted components have the longer lifetime or by a relaxation model in which the spectrum shifts to longer wavelength as time evolves due to reorientation of polar moieties of the protein about the chromophore (Lakowicz & Cherek, 1980). If the former model is correct, and if different ground-state species have distinct absorption spectra, it should be possible to selectively excite particular species. We are currently studying the dependence of the emission decay on the excitation frequency in an attempt to decide between these alternative explanations.

Table V includes values for the average lifetimes of Trp-3 in $proPLA_2$ and PLA_2 at 8, 20, and 40 °C calculated from the lifetime data. In a well-behaved photophysical system with a fixed fluorophore radiative rate constant, the ratio of the lifetime (or average lifetime) to the quantum yield is constant. A comparison of the average lifetimes at 20 °C with the quantum yields listed in Table I indicates that there are discrepancies between these two sets of measurements. For $proPLA_2$ vs. PLA_2 the ratio of quantum yields is 3.0 while the ratio of average lifetimes is 2.2, and for $PLA_2/C_{16}PN$ vs. PLA_2 the ratios are 2.4 vs. 1.4. These results can be rationalized by assuming that a fraction of the tryptophans in the sample are nonfluorescent. This fraction can be calculated from the equation (Hazan et al., 1976) $F_{nf} = 1 - (Q/Q_s)(\tau_s/\langle\tau\rangle)$, where Q is the quantum yield of the protein, Q_s is the quantum yield of a standard, τ_s is the lifetime of the standard, and $\langle\tau\rangle$ is the average lifetime of the protein. Values of F_{nf} calculated in this manner from the data in Tables I and III using a lifetime of 3.0 ns for NATA (Szabo & Rayner, 1980; Ross et al., 1981a; Petrich et al., 1983) are 0.51 for PLA_2, 0.33 for $proPLA_2$, and 0.13 for $PLA_2/C_{16}PN$.

It appears that the emission of Trp-3 in PLA_2 simplifies to a double-exponential decay when the protein forms a complex with the substrate analogue $C_{16}PN$. This result may reflect a change in the environment of Trp-3 in the complex. If the indole ring is transferred into the hydrophobic environment of the micellar acyl chains, as the data in Table I indicate, then the simpler decay kinetics may reflect a more homogeneous environment of the ring in the complex. The two remaining lifetimes may be just the limiting number found for nearly all tryptophan derivatives. Anisotropy decay studies (Ludescher et al., 1986) provide evidence that the tryptophan ring is nearly immobile in the complex. The decrease in the number of lifetimes may also reflect this immobility, with the ring sampling fewer environments during its excited-state lifetime.

With all of these observations in mind we present a description of the behavior of tryptophan in this protein that is more general than a decomposition into discrete lifetime components. What we propose is that the excited-state decay behavior of proteins in general, and PLA_2 in particular, is best represented as a distribution of decay rates. Thermal population of a variety of ring orientations and protein conformations must result in a continuous distribution of species with an associated distribution of excited-state decay constants. This variation in decay rates is probably due primarily to variation in radiationless decay processes. Furthermore, the rate of interchange between these individual "microenvironments" probably occurs on the time scale of the excited-state population decay so that the lifetime is modulated by thermal motion after excitation (Ludescher et al., 1986). This description leaves open the question of whether the excitation process, and the resulting change in the electronic distribution of the indole chromophore, modifies the configurational energies and interchange rates so that they are different from the ground-state behavior.

According to this description of the heterogeneity of the decay behavior of tryptophan in proteins, the representation of the time dependence of the emission as a discrete set of exponential decays is an approximation that reveals the moments of the underlying distribution. In simulation calculations we have shown that a Gaussian distribution of lifetimes, when convoluted with a real instrument response function and then fit to exponentials, is very well represented by a discrete set of exponential decays. As might be anticipated, the criteria used in this study to determine the requisite number of decays indicate that a single exponential adequately represents a narrow Gaussian distribution while two or more "components" are needed for broad distributions. The resulting discrete set of exponentials reproduce the mean and width of the input distribution.

The question of how many exponential components are needed to represent a data set is converted, according to this continuous picture, to the question of how detailed a description of the distribution of decays can be extracted from the given data. If, as seems likely, the decays are distributed according to some simple functional form, then a few terms will be

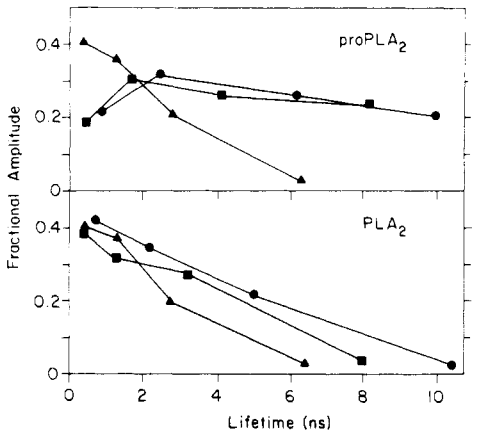

FIGURE 4: Lifetime distribution spectra of $proPLA_2$ and PLA_2. The amplitudes of Table V are plotted as a function of the observed lifetime at 8 (circles), 20 (squares), and 40 °C (triangles).

adequate to provide the parameters of the distribution. On the other hand, the inclusion of more than the minimum number of terms needed to describe the data will probably not significantly influence the lower order moments of the distribution. It should be emphasized that if the decay is continuously distributed, then the parameters deduced from any finite exponential approximation do not represent physically defined processes or concentrations of species. The physically significant quantities are the mean value, the dispersion, and higher moments of the distribution.

The graphical representations of the lifetime data presented in Figure 4 can be thought of as approximations to this continuous distribution function. Similarly, the numbers given in the last two columns of Table V are the mean and standard deviation of these lifetime distributions. These mean and dispersion values are essentially independent of the number of lifetime components in the analysis so long as that number is at least three; two-component fits give significantly different values, and five-component fits reproduce the results of the four-component analysis.

Several features of these distributions are of interest. The first is that the width of the distribution is comparable to the mean value. The considerable dispersion is, of course, the reason that the data require three or more components for adequate fits. The form of these distributions is also of interest. The general shape seems to be that of a continuous decrease from low lifetimes. It should be remembered in this context that the comparison of quantum yield and lifetime measurement presented above indicates that there is a significant fraction of the protein with effectively a zero lifetime. The inclusion of this component would further increase these curves at the short time end. Another point of interest is that the standard deviation of the lifetime distributions (Table V) is decreased as the temperature is increased. On the other hand, the ratio of the standard deviation to the mean lifetime remains essentially constant. This pattern is consistent with a thermal interconversion between environments with widely different decay rates.

The time-resolved fluorescence measurements described here demonstrate that the excited-state decay behavior of tryptophan in proteins is, at least in this case, far more complicated than previously reported. The decay kinetics of the single tryptophan in both $proPLA_2$ and PLA_2 require at least three exponentials for an adequate description. This finding is certainly not surprising considering the extraordinary complexity of the photophysics of the indole chromophore and the double-exponential decay kinetics of free tryptophan amino acid. The best description of the behavior of tryptophan in these proteins appears to be that there is a continuous distribution of decay rates with interchange between the subenvironments.

ACKNOWLEDGMENTS

R.D.L. is especially grateful to Enoch Small and Louis Libertini for their technical expertise and patient assistance. Their contribution was essential to the successful completion of this work. He is also thankful for many helpful discussions with Anthony Ruggiero, Duane Flamig, and the late Irvin Isenberg. We thank Suzanne Hudson for expert assistance in computer programming and Mary Gilland for assistance in the preparation of the figures. We also thank Enrico Gratton and Franklyn Prendergast for communication of the results of experiments prior to publication.

Registry No. PLA_2, 9001-84-7; $proPLA_2$, 37350-21-3; $C_{16}PN$, 93597-88-7; NATA, 1218-34-4; L-Trp, 73-22-3.

REFERENCES

Andrews, L. J., & Forster, L. S. (1974) *Photochem. Photobiol. 19*, 353.
Bent, D. V., & Hayon, E. (1975) *J. Am. Chem. Soc. 97*, 2612.
Bevington, P. V. (1969) *Data Reduction and Error Analysis for the Physical Sciences* McGraw-Hill, New York.
Brochon, J. C., Wahl, P., Charlier, M., Maurizot, J. C., & Helene, C. (1977) *Biochem. Biophys. Res. Commun. 79*, 1261.
Brockerhoff, H. (1968) *Biochim. Biophys. Acta 159*, 296.
Brockerhoff, H. (1973) *Chem. Phys. Lipids 10*, 215.
Burstein, E. A., Vedenkina, N. S., & Ivkova, M. N. (1973) *Photochem. Photobiol. 18*, 263.
Chang, M. C., Petrich, J. W., McDonald, D. B., & Fleming, G. R. (1983) *J. Am. Chem. Soc. 105*, 3819.
Chen, R. F. (1972) *J. Res. Natl. Bur. Stand., Sect. A 76A*, 593.
Cockle, S. A., & Szabo, A. G. (1981) *Photochem. Photobiol. 34*, 23.
Cowgill, R. W. (1963) *Arch. Biochem. Biophys. 100*, 36.
Dijkstra, B. W., Kalk, K. H., Drenth, J., & Vandermaelen, P. J. (1978) *J. Mol. Biol. 124*, 53.
Dijkstra, B. W., Drenth, J., & Kalk, K. H. (1981a) *Nature (London) 289*, 604.
Dijkstra, B. W., Kalk, K. H., Hol, W. G. J., & Drenth, J. (1981b) *J. Mol. Biol. 147*, 97.
Dijkstra, B. W., van Nes, G. J. H., Kalk, K. H., Brandenberg, N. P., Hol, W. G., & Drenth, J. (1982) *Acta Crystallogr., Sect. B: Struct. Crystallogr. Cryst. Chem. B38*, 793.
Eftink, M., & Ghiron, C. A. (1976) *Biochemistry 15*, 672.
Eisinger, J., & Navon, G. (1969) *J. Chem. Phys. 50*, 2069.
Feitelson, J. (1971) *Photochem. Photobiol. 13*, 2612.
Fletcher, R., & Powell, M. J. D. (1963) *Comput. J. 6*, 163.
Grinvald, A., & Steinberg, I. Z. (1974) *Anal. Biochem. 54*, 583.
Grinvald, A., & Steinberg, I. Z. (1976) *Biochim. Biophys. Acta 427*, 663.
Gudgin, E., Lopez-Delgado, R., & Ware, W. R. (1981) *Can. J. Chem. 59*, 1037.
Hazan, G., Haas, E., & Steinberg, I. Z. (1976) *Biochim. Biophys. Acta 434*, 144.
Himmelblau, D. M. (1972) *Applied Nonlinear Programming*, McGraw-Hill, New York.
Isenberg, I. (1973a) *J. Chem. Phys. 59*, 5696.
Isenberg, I. (1973b) *J. Chem. Phys. 59*, 5708.

Isenberg, I. (1983) *Biophys. J. 43*, 141.
Isenberg, I., Dyson, R. D., & Hanson, R. (1973) *Biophys. J. 13*, 1090.
Jansen, E. H. J. M. (1979) Ph.D. Dissertation, State University at Utrecht, The Netherlands.
Joschek, H.-I., & Grossweiner, L. I. (1966) *J. Am. Chem. Soc. 88*, 3261.
Kirby, E. P., & Steiner, R. F. (1970) *J. Phys. Chem. 74*, 4480.
Konev, S. V. (1967) *Fluorescence and Phosphorescence of Proteins and Nucleic Acids*, Plenum Press, New York.
Lakowicz, J. R. (1983) *Principles of Fluorescence Spectroscopy*, Plenum Press, New York and London.
Lami, H. (1977) *J. Chem. Phys. 67*, 3274.
Lasser, N., Feitelson, J., & Lumry, R. (1977) *Isr. J. Chem. 16*, 330.
Lehrer, S. S. (1976) in *Biochemical Fluorescence: Concepts* (Chen, R. F., & Edelhoch, H., Eds.) Vol. 2, pp 515–544, Marcel Dekker, New York, Basel.
Longworth, J. W. (1971) in *Excited States of Proteins and Nucleic Acids* (Steiner, R. F., & Weinryb, I., Eds.) pp 319–484, Plenum Press, New York and London.
Ludescher, R. D., Volwerk, J. J., de Haas, G. H., Jost, P. C., & Hudson, B. (1986) *Biochemistry* (submitted for publication).
Lumry, R., & Hershberger, M. (1978) *Photochem. Photobiol. 27*, 819.
Lumry, R., Yanari, S., & Bovey, F. A. (1962) *Pap. Meet.—Am. Chem. Soc., Div. Org. Coat. Plast. Chem.*, 18R (Reprint 142).
Marquadt, D. W. (1963) *J. Soc. Ind. Appl. Math. 11*, 431.
Nieuwenhuizen, W., Kunze, H., & de Haas, G. H. (1974) *Methods Enzymol. 32B*, 147.
Petrich, J. W., Chang, M. C., McDonald, D. B., & Fleming, G. R. (1983) *J. Am. Chem. Soc. 105*, 3824.
Pieterson, W. A., Vidal, J. C., Volwerk, J. J., & de Haas, G. H. (1974) *Biochemistry 13*, 1455.
Privat, J.-P., Wahl, P., & Auchet, J.-C. (1980) *Biophys. Chem. 11*, 239.
Roberts, M. F., Deems, R. A., & Dennis, E. A. (1977) *Proc. Natl. Acad. Sci. U.S.A. 74*, 1950.
Ross, J. B. A., Rousslang, K. W., & Brand, L. (1981a) *Biochemistry 20*, 4361.
Ross, J. B. A., Schmidt, C. J., & Brand, L. (1981b) *Biochemistry 20*, 4369.
Slotboom, A. J., & de Haas, G. H. (1975) *Biochemistry 14*, 5394.
Slotboom, A. J., Jansen, E. H. J. M., Pattus, F., & de Haas, G. H. (1978) in *Semisynthetic Peptides and Proteins* (Offord, R. E., & DiBello, C., Eds.) Academic Press, New York, London, and San Francisco.
Small, E. W., & Isenberg, I. (1976) *Biopolymers 15*, 1093.
Small, E. W., & Isenberg, I. (1977) *J. Chem. Phys. 66*, 3347.
Small, E. W., Libertini, L., & Isenberg, I. (1984) *Rev. Sci. Instrum. 55*, 879.
Strickland, E. H., Horwitz, J., & Billups, C. (1970) *Biochemistry 9*, 4914.
Szabo, A. G., & Rayner, D. M. (1980) *J. Am. Chem. Soc. 102*, 554.
Szabo, A. G., Stepanik, T. M., Wayner, D. M., & Young, N. M. (1983) *Biophys. J. 41*, 233.
Tinker, D. O., Low, R., & Lucassen, M. (1980) *Can. J. Biochem. 58*, 898.
Valeur, B., & Weber, G. (1977) *Photochem. Photobiol. 25*, 441.
Van Dam-Mieras, M. C. E., Slotboom, A. J., Pieterson, W. A., & de Haas, G. H. (1975) *Biochemistry 14*, 5387.
van Scharrenburg, G. J. M., Puijk, W. C., Egmond, M. R., van der Schaft, P. H., de Haas, G. H., & Slotboom, A. J. (1982) *Biochemistry 21*, 1345.
Verger, R., Mieras, M. C. E., & de Haas, G. H. (1973) *J. Biol. Chem. 248*, 4023.
Volwerk, J. J., & de Haas, G. H. (1982) in *Lipid-Protein Interactions* (Jost, P., & Griffith, O. H., Eds.) Vol. 1, pp 69–149, Wiley, New York.
Walker, M. S., Bednar, T. W., & Lumry, R. (1967) *J. Chem. Phys. 47*, 1020.
Weinryb, I., & Steiner, R. F. (1971) in *Excited States of Proteins and Nucleic Acids* (Steiner, R. F., & Weinryb, I., Eds.) pp 277–318, Plenum Press, New York and London.
Wells, M. A. (1978) in *Advances in Prostaglandin and Thromboxane Research* (Galli, C., et al., Eds.) Vol. 3, pp 39–45, Raven Press, New York.
Yamamoto, Y., & Tanaka, J. (1972) *Bull. Chem. Soc. Jpn. 45*, 1362.